Detailed spectroscopy of ^{249}Fm

A. Lopez-Martens,[1] K. Hauschild,[1] A. V. Yeremin,[2] A. V. Belozerov,[2] Ch. Briançon,[1] M. L. Chelnokov,[2] V. I. Chepigin,[2] D. Curien,[3] O. Dorvaux,[3] B. Gall,[3] V. A. Gorshkov,[2] M. Guttormsen,[4] F. Hanappe,[5] A. P. Kabachenko,[2] F. Khalfallah,[3] A. Korichi,[1] A. C. Larsen,[4] O. N. Malyshev,[2] A. Minkova,[6] Yu. Ts. Oganessian,[2] A. G. Popeko,[2] M. Rousseau,[3] N. Rowley,[3] R. N. Sagaidak,[2] S. Sharo,[7] A. V. Shutov,[2] S. Siem,[4] A. I. Svirikhin,[2] N. U. H. Syed,[4] and Ch. Theisen[8]

[1]*CSNSM, IN2P3-CNRS, F-91405 Orsay Campus, France*

[2]*FLNR, JINR, Dubna, Russia*

[3]*IPHC, IN2P3-CNRS, F-67037 Strasbourg, France*

[4]*Department of Physics, Oslo University, N-0316 Oslo, Norway*

[5]*Université Libre de Bruxelles, B-1050 Bruxelles, Belgium*

[6]*Department of Atomic Physics, University of Sofia, BG-1164 Sofia, Bulgaria*

[7]*Department of Physics, Comenius University, SK-84215, Bratislava, Slovakia*

[8]*DAPNIA/SPhN, CEA-Saclay, France*

(Received 10 March 2006; revised manuscript received 19 July 2006; published 4 October 2006)

Excited states in ^{249}Fm were populated via the α decay of ^{253}No and the subsequent decay was observed with the GABRIELA detection system installed at the focal plane of the VASSILISSA recoil separator. The energies, spins, and parities of these states could be established through combined α, γ, and conversion-electron spectroscopy. The first members of the ground-state rotational band were identified. Their excitation energies as well as the observation of a cross-over $E2$ transition confirm the assignment of $7/2^+$ [624] for the ground state of ^{249}Fm. Two excited states were also observed and their decay properties suggest that they correspond to the particle excitation $9/2^-$ [734] and hole excitation $5/2^+$ [622]. The analysis suggests that the 279-keV transition de-exciting the $9/2^-$ state has anomalous $E1$ conversion coefficients.

DOI: 10.1103/PhysRevC.74.044303 PACS number(s): 23.20.Lv, 23.20.Nx, 23.60.+e, 27.90.+b

I. INTRODUCTION

Elements beyond Fm (proton number $Z = 100$) owe their existence solely to quantal effects. These effects are enhanced when the neutron and proton configurations coincide with shell-like structures that result from the underlying mean field. The predicted stability, deformation and structure of heavy elements is therefore extremely model dependent. A systematic investigation of heavy nuclei with $Z \geqslant 100$ is the only way to constrain the models and test their reliability. The study of odd-mass isotopes is particularly revealing since it can give direct information on the nature and sequence of the single-particle states around the Fermi surface.

Structural information on odd-N and odd-Z transfermium nuclei has been obtained essentially from α-decay studies [1]. The early results of Bemis *et al.* [2] on the decay of ^{255}No represent the first investigations above proton number $Z = 100$ where α spectroscopy with coincident detection of x rays and low-energy photons was used. However, it is only recently that investigations of transfermium elements systematically combine α-decay studies with γ spectroscopy, making it possible to obtain high-resolution information on nuclear level energies in the daughter nuclei. Such studies have been performed in ^{251}No [3], ^{247,249}Fm [4], and ^{255}Fm [5] and have shed some light on the nature of the first excited states in these nuclei, as well as on the nature of the ground states and isomeric states of their parents. Higher spin states can be accessed via in-beam γ-ray spectroscopy. The recent leap forward in this area is related to the use of efficient 4π germanium arrays combined with recoil separators. As an example, the electric quadrupole ($E2$) transitions de-exciting the high-spin members of an excited rotational band in ^{253}No [6] were observed using Gammasphere [7] and the FMA [8]. The small interband $M1$ branch responsible for the observation of the rotational band suggests that the configuration of the band most likely is the $7/2^+$[624] neutron orbital stemming from the $g_{9/2}$ spherical orbital. The odd-Z isotopes ^{251}Md [9] and ^{255}Lr [10] have also been studied in a similar way with Jurogam and the RITU spectrometer [11] at Jyväskylä. Further, less ambiguous information on the spin and parity of nuclear levels can be obtained by internal-conversion-electron spectroscopy, especially since internal conversion can compete with, and even dominate, electromagnetic radiation in this mass region. α spectroscopy combined with γ and conversion-electron spectroscopy has been carried out in ^{249}Fm [12] and ^{253}Fm [13]. In the latter case, the observed sequence of excited states in ^{253}Fm and their corresponding population from the ground state of ^{257}No suggest that ^{257}No breaks the $N = 155$ isotonic trend in that its ground state is assigned to be the $3/2^+$[622] configuration instead of the $7/2^+$[613]. In the case of ^{249}Fm, γ rays and conversion electrons were observed by Herzberg *et al.* [12] and the decay of an excited state assigned to the $9/2^-$[734] configuration was identified. However, no other excited states were directly observed and no values for the conversion coefficients of the identified transitions were given in Ref. [12]. We report here on a new measurement involving the detection of γ rays and internal-conversion electrons in the decay of excited states in ^{249}Fm.

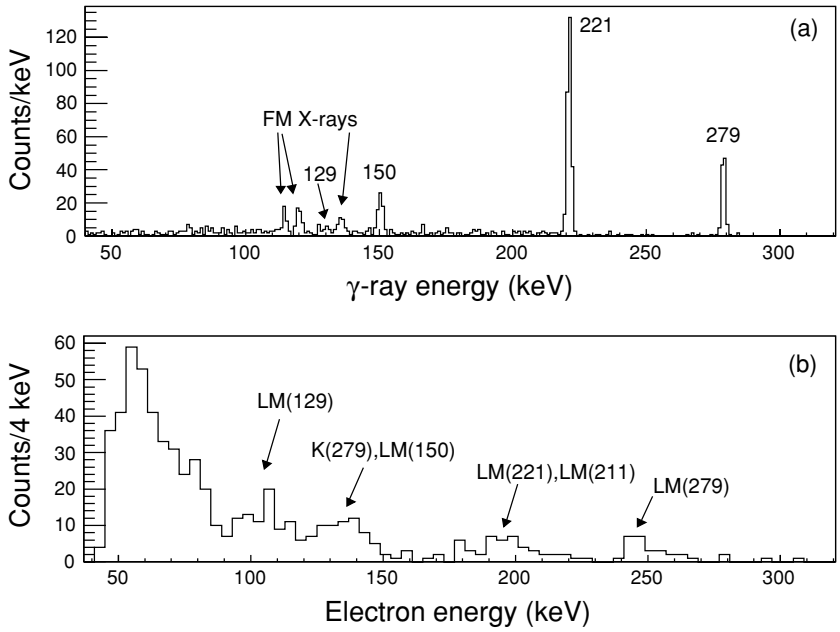

FIG. 1. (a) Compton-suppressed energy spectrum of γ rays detected in prompt coincidence with the ^{253}No α decay. (b) Energy spectrum of conversion electrons following the α decay of ^{253}No.

II. EXPERIMENTAL TECHNIQUES AND RESULTS

Excited states in ^{249}Fm were populated via the α decay of ^{253}No, which was produced in the reaction ^{207}Pb(^{48}Ca, $2n$). The 0.7-pμA ^{48}Ca beam was provided by the U400 cyclotron of the FLNR, JINR, Dubna. The 350 μg/cm^2 PbS targets were mounted on a rotating target frame to avoid melting of the target. The fusion-evaporation residues [mainly the two-neutron-evaporation channel ($2n$) into ^{253}No but also the $1n$ and $3n$ channels into ^{254}No and ^{252}No, respectively] were transported by the VASSILISSA separator [14,15] and implanted into the stop detector of the GABRIELA detection system [16] installed at the focal plane of the separator. The energy calibration of the backward electron detectors (tunnel) was performed by producing and implanting ^{207}Rn recoils in an isomeric state that is known to decay via internal-conversion-electron emission [17]. In this way, correction could be made for the energy loss of the electrons in the stop detector. From detailed simulations of the GABRIELA setup [16], it is estimated that the energy deposition in the stop detector by electrons that escape backward is less than 3 keV for electron energies ranging from 50 to 300 keV and for an average implantation depth of 2 μm.

From their decay properties, it is difficult to distinguish ^{253}No from ^{254}No recoils: Their lifetimes differ only by a factor of $\sim$2 (96 and 55 s, respectively) and the energy of the ^{254}No α decay (8.1 MeV) coincides with the energy range of the ^{253}No α group. From previously measured $1n$ and $2n$ excitation functions, it was not possible to determine how much ^{254}No was actually produced in the reaction since the uncertainty in the measurement of the beam energy was of the order of 1.5 MeV. Nevertheless, the presence of ^{254}No does not affect the analysis described here since, during a dedicated run with a ^{208}Pb target, the ground state of ^{254}No was observed to decay mainly to the ground state of ^{250}Fm with no coincident emission of γ rays or conversion electrons. However, the presence of ^{254}No makes it impossible to determine the absolute branching ratios from the ground state of ^{253}No to the levels in ^{249}Fm.

A. γ and electron spectroscopy

A total of 10,500 α particles from the decay of ^{253,254}No were detected during the experiment. No delayed γ or electron emission following the α decay of ^{253}No was observed. The spectra of γ rays and conversion electrons detected in prompt coincidence with the ^{253}No α emission are shown in Fig. 1. In the top panel of Fig. 1, three γ lines at 150, 221, and 279 keV are clearly visible as well as Fm x rays at 115, 121, and 136–141 keV. No coincidences between the most intense lines at 221 and 279 keV are observed, which means that they do not form a cascade. The electron spectrum shows structures around 55, 65, 80, 100, 135, 200, and 250 keV. In the γ-electron matrix of Fig. 2, low-energy electrons of $\sim$55 keV are observed to be in coincidence with the 150- and 221-keV γ transitions and $\sim$70-keV electrons are coincident with the 150-keV transition. The singles spectrum of γ rays observed in this work is similar to those observed in the experiments performed by Hessberger *et al.* [4] and by Herzberg *et al.* [12].

B. α-γ spectroscopy

Figure 3(b) shows the prompt α-γ correlations detected in the experiment. At first sight, it seems that the 279- and 221-keV γ rays are correlated to different α decays of ^{253}No. This is more clearly shown in Figs. 4(a) and 4(b), where the energy spectra of the α particles in coincidence with both γ rays are displayed: The α-particle energy spectrum in coincidence with the 221-keV γ ray is shifted by approximately

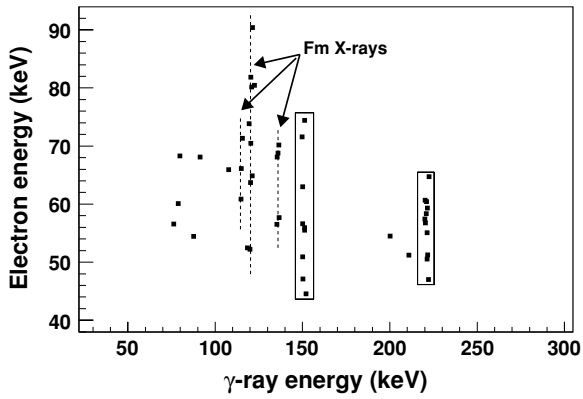

FIG. 2. γ-electron coincidence matrix. The conversion electrons detected in coincidence with the 150- and 221-keV γ rays are surrounded by boxes.

50 keV compared to the one in coincidence with the 279-keV transition.

This effect can be explained by the the fact that the 221-keV γ ray is in coincidence with a highly converted transition. The energies of the internal-conversion electrons and associated x rays and Coster-Kronig and Auger electrons emitted in the internal-conversion process are summed (totally or partially) with the α-particle energy in the implantation detector. This explanation is verified with the energy spectrum of α particles detected in coincidence with the 221-keV γ ray as well as with a conversion electron in the tunnel [see Fig. 4(c)]. The statistics are poor, but it is clear that the centroid of the distribution of counts lies at lower energies than when no coincident electron is required [Fig. 4(b)].

From Fig. 4(a), the energy of the α particle populating the 279-keV transition is extracted to be 8003(5) keV. If the highest energy peak at 8280(10) keV in the α spectrum shown in Fig. 3(a) is assumed to populate the ground state of ^{249}Fm, then the 279-keV transition must be a transition to the ground state of ^{251}Fm.

If the 221-keV γ ray is also fed by the 8003(5)-keV α decay, the summing effects discussed earlier are due to

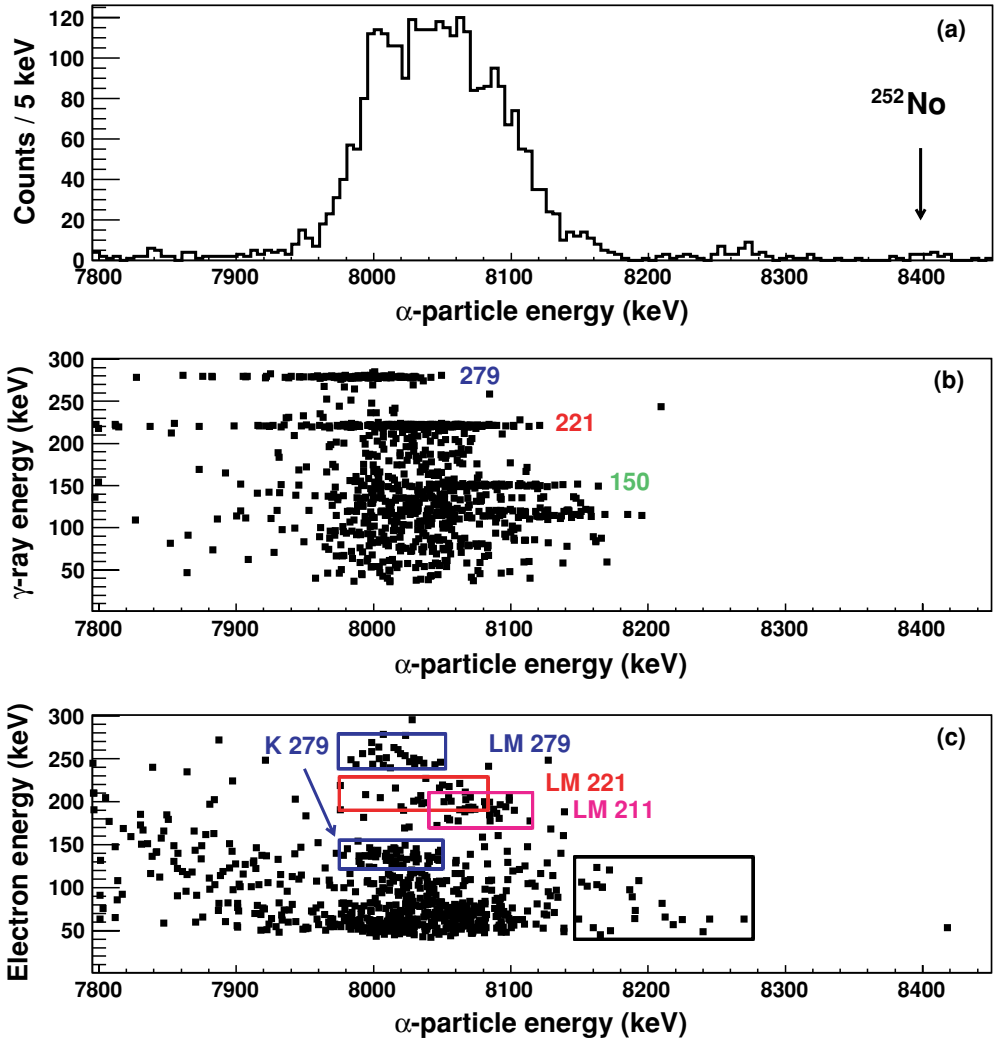

FIG. 3. (Color online) (a) Energy spectrum of recoil-position-correlated α particles. (b) Spectrum of prompt α-γ and (c) α-electron coincidences as a function of α-particle energies and γ-ray or conversion-electron energies. The boxes are to guide the eye (see text).

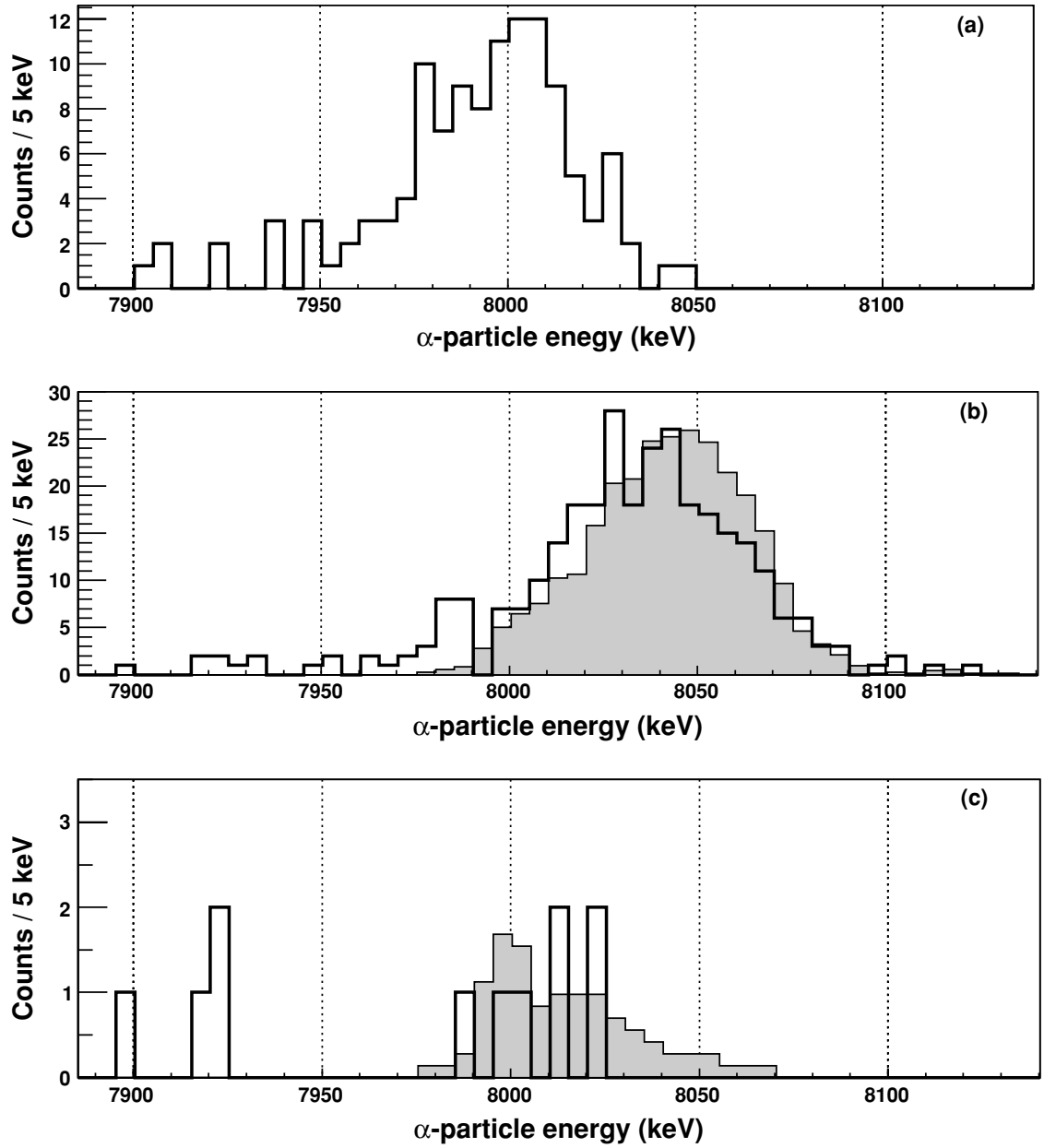

FIG. 4. Energy spectrum of α particles detected in coincidence with (a) the 279-keV γ ray, (b) the 221-keV γ ray, and (c) the 221-keV γ ray with the extra requirement that an electron is detected in the tunnel detector. The shaded histograms in panels (b) and (c) represent the result of GEANT4 Monte Carlo simulations.

the conversion of a 58-keV transition. This fits well with the fact that ~55-keV electrons are detected in coincidence with the 221-keV γ ray (see Fig. 2). To verify this scenario, GEANT4 Monte Carlo simulations [18] were performed. In these simulations, recoils are implanted at a depth of 2 μm into the stop detector. Conversion electrons and subsequent x-ray and Auger electrons are emitted by the recoils into 4π and detected either in the stop detector or in the tunnel detectors. The relevant fluorescence yields for vacancies in the K and L atomic shells are taken from Ref. [19]. The x-ray energies are determined from differences between the corresponding atomic-shell binding energies and x-ray intensities per K- or L-shell vacancies are taken from Refs. [19,20]. The simulation of the multiple processes stemming from the creation of vacancies in the M and higher atomic shells is performed via the emission of a single electron carrying all the remaining energy. This is a valid approximation since, for ^{249}Fm ($Z = 100$), the remaining energy is less than the binding energy of the M shell (<8 keV) and therefore always fully absorbed in the stop detector. The resolution of the stop detector is taken to be 30 keV. Knowledge of the multipolarity of the 58-keV transition is not crucial, since L conversion is the dominant process for $E1$, $E2$, and $M1$ transitions. Furthermore, although the fluorescence yield of the $L1$ shell is half that of the $L2$ and $L3$ shells, this lack of x-ray yield is compensated by a large Coster-Kronig probability leading to

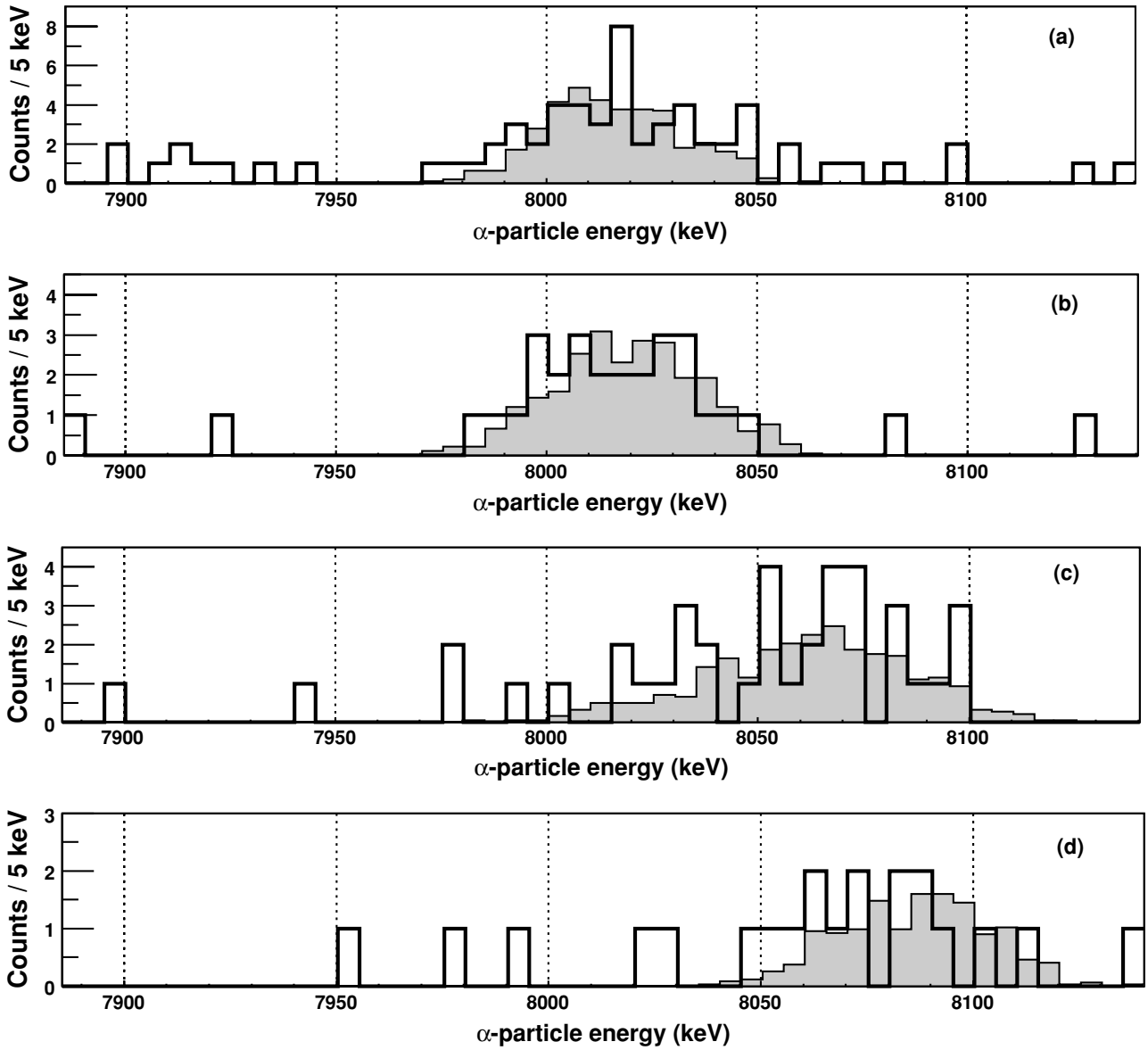

FIG. 5. Energy spectrum of α particles detected in coincidence with (a) the K-conversion electrons of the 279-keV transition, (b) the LMN-conversion electrons of the 279-keV transition, (c) the LMN-conversion electrons of the 221-keV transition, and (d) the LMN-conversion of the 211-keV transition. In each panel, the shaded histogram corresponds to the simulated α-particle energy spectrum.

$L3$ vacancies. For vacancies in the K shell, the fluorescence yield is taken to be 1.

The results of the simulation for the α-particle energy spectrum detected in coincidence with the 221-keV γ ray and for the α-particle energy spectrum detected in coincidence with the 221-keV γ ray and with electrons of energy higher than 40 keV (as in the experiment) are displayed as shaded histograms in Figs. 4(b) and 4(c). Given the uncertainties of up to $\sim$20% in the fluorescence yields in heavy elements, there is a qualitatively good agreement between the simulations and the experimental data. This consistency supports the picture in which both the 279- and 221-keV transitions are correlated to the same α particle, which feeds a level in ^{251}Fm at 279-keV excitation energy.

In Refs. [4,12], it was suggested that the 150-keV transition also depopulates the 279-keV level. This would imply the existence of a state at 129-keV excitation, which decays to the 58-keV level via a 71-keV transition. This scenario is confirmed by the fact that the 150-keV line is coincident with $\sim$55- and $\sim$70-keV electrons and by the presence of a structure at 100 keV in the electron singles spectrum of Fig. 1(c). This structure corresponds to the $LMN+$ conversion of a 129-keV transition, which is barely visible in the singles γ-ray spectrum just below the Fm K_β x rays at $\sim$136keV. Furthermore, there is direct population of the 58- and 129-keV levels in the α decay of ^{253}No since α-electron coincidences are recorded at the expected electron and α-particle energies [see the box in Fig. 3(c) at α-particle energies larger than 8150 keV].

As discussed previously, because of summing in the stop detector, part of the coincident α particles will be detected with apparent energies higher than the true energies.

C. α-electron spectroscopy

The electron structure visible at the highest energies in Fig. 1(b) is most probably the $LMN+$ conversion of the 279-keV transition since the energy difference between it and 279 keV is similar to the average binding energy of the L and M atomic shells in ^{251}Fm. The α-particle energy spectrum in coincidence with these electrons is shown in Fig. 5(b). The result of the Monte Carlo simulation assuming that these electrons do indeed correspond to the $LMN+$ conversion of the 279-keV transition is also displayed and supports the assignment of the 250-keV electron structure to the $LMN+$ conversion of the 279-keV transition.

K-conversion electrons of the 279-keV transition are expected to have energies around 137 keV. In Fig. 3(c), a cluster of electrons is clearly visible at electron energies between 120 and 150 keV. The energies of the α particles in coincidence with this cluster of electrons is shown in Fig. 5(a) together with the output of the corresponding GEANT4 simulation. The simulation of the energy deposition in the stop detector by x rays and auger electrons following the K conversion of the 279-keV transition describes the experimental data well. There is some intensity at α-particle energies greater than 8050 keV, which is not accounted for by the simulation. This contamination is due to the LMN conversion of the 150-keV transition. However, since the 150-keV γ-ray line is mainly coincident with α particles of energies greater than 8050 keV [see Fig. 3(b)], the corresponding LMN-conversion electrons should not contribute significantly to the experimental spectrum of Fig. 5(a) below 8050 keV.

The LMN-conversion electrons associated with the 221-keV transition should have energies between 190 and 220 keV. One might be tempted to associate the 200-keV electron structure to the LMN conversion of the 221-keV transiton. However, by inspection of the singles electron spectrum of Fig. 1(b), the electron structure at 200 keV is seen to extend down to energies lower than expected for the $LMN+$ conversion of a single transition of 221 keV given the experimental resolution of $\sim$10–12 keV. Furthermore, the boxes drawn in Fig. 3(c) at electron energies around 200 keV reveal that the lower-energy part of the 200-keV electron structure is in coincidence with higher-energy α-particles than the higher-energy part of the electron structure.

The energy spectrum of the α particles in coincidence with the higher energy electrons ($>$190 keV) is displayed in Fig.5(c). It coincides well with the simulation of the 221- to 58-keV cascade requiring the detection of the LMN-conversion electrons of the 221-keV transition in the tunnel detectors.

The energy spectrum of α particles in coincidence with the lower energy part of the electron structure (which is displaced by $\sim$10 keV with respect to the higher energy part) is shown in Fig. 5(d). It is best described as the conversion of a single 211(5)-keV transition to the ground state of ^{251}Fm in coincidence with an α particle of 8070(10) keV.

D. Internal-conversion coefficients

Given that absolute efficiencies for detecting γ rays and electrons were measured for GABRIELA [16], internal-conversion coefficients could be extracted for the 129-, 150-, 211-, 221-, and 279-keV γ lines. These experimental values were then compared to the theoretical values for $E1$, $E2$, or $M1$ transitions obtained with a computer program based on Refs. [21,22]. In the transition-energy range of interest, no important differences were found between the theoretical coefficients of [21,22] and the more recent values tabulated in [23]. The precision of the measurement of the $LMN+$-conversion coefficient does not allow a discrimination between $M1$ or $E2$ character for the 129-keV transition; however, from the distribution of intensity within the 100-keV electron structure, it is likely that the 129-keV transition is mostly of $E2$ nature since $\alpha_{L2} > \alpha_{L3} > \alpha_{L1}$. The conversion coefficients for the 129-, 150-, 211-, 221-, and 279-keV transitions are presented in Fig. 6. Two counts are recorded at γ-ray energies $\sim$211 keV and α energies between 8050 and 8090 keV, which allows for an estimation of the $LMN+$-conversion coefficient of the 211-keV transition. A value of 2.8(2.2) is found, which indicates that the 211-keV transition is very probably an $M1$, or an $E2$, or a mixed $M1$-$E2$ transition. The $E1$ character of the 150- and 221-keV transitions is firmly established and is

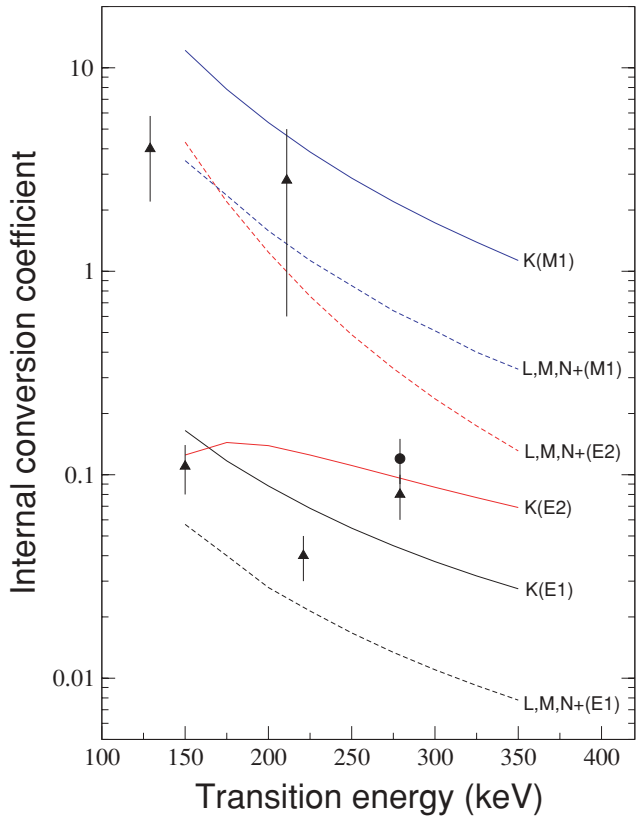

FIG. 6. (Color online) The theoretical internal-conversion coefficients (lines) for Fm isotopes as a function of transition energy based on Ref. [21] for K, L, and M and on Ref. [22] for $N+$. The filled triangles correspond to the experimentally determined $LMN+$ coefficients and the filled circle is the K-conversion coefficient measured for the 279-keV transition.

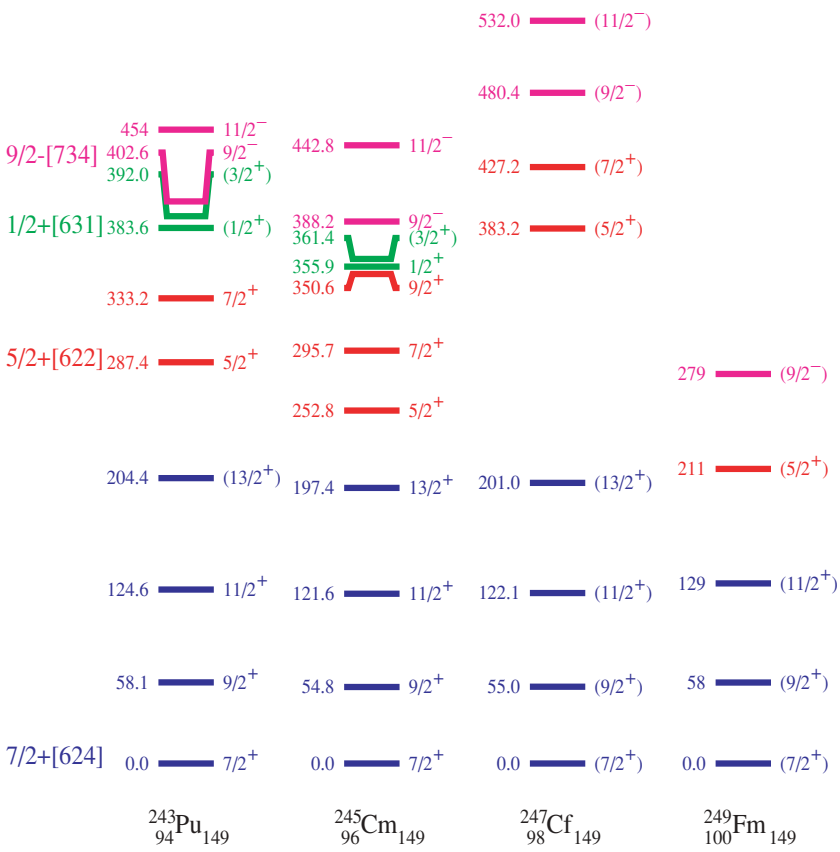

FIG. 7. (Color online) Experimental systematics of low-lying levels in $N = 149$ isotones taken from [31] and based on the present data.

consistent with the conclusion of previous work [4,12]. The picture, however, is not quite as clear-cut for the 279-keV transition since the K- and $LMN+$-conversion coefficients are systematically much higher than the theoretical values for $E1$ transitions.

A possible explanation for the large $E1$ conversion of the 279-keV transition could be the large conversion of a weak γ transition of similar energy. However,such anomalous $E1$ conversion is not uncommon in heavy deformed nuclei (cf. Appendix D of Ref. [24] and references therein). This phenomenon occurs in the case of transitions for which the γ-ray matrix element is inhibited while the usually negligible penetration matrix elements are not and may therefore produce sizable deviations from the tabulated internal-conversion coefficients [25,26]. To disentangle these two scenarios, it is useful to examine the x rays detected in coincidence with the ^{253}No α decay. The x-ray intensity observed in Fig. 1(a) is of the order of a factor 2.0(0.3) higher than the expected x-ray intensity from the K conversion of the 150-, 221-, and 279-keV transitions, assuming they are all $E1$ transitions and taking the theoretical K-conversion coefficients. Such a high x-ray intensity can also be deduced from the large values of the upper limits for the K-conversion coefficients shown in Table 1 of Ref. [4]. If one takes the measured K-conversion coefficient for the 279-keV transition, the x-ray intensity is still 1.5(0.3) times higher than what it should be. However, if the K conversion of the 211-keV transition is taken into account, assuming it is mainly an $M1$ transition, the discrepancy between the emitted number of K electrons and the emitted number of x rays practically vanishes. This observation supports the anomalous $E1$ conversion of the 279-keV transition as well as the presence of the 211-keV transition.

III. DISCUSSION

For relatively low energy levels of odd-mass deformed nuclei, the component of the total angular momentum I on the symmetry axis, K, is equal to Ω, the projection of the angular momentum of the odd particle. Furthermore, on top of each intrinsic state, a rotational band with spin sequence $K, K+1, K+2, \ldots$ can be built. In the case of $K \neq 1/2$, the excitation energy of the band member of spin I is given by $E(I) = E_0 + \hbar^2/2\Im I(I+1)$, where E_0 is the bandhead energy and $\Im$ is the nuclear moment of inertia about an axis perpendicular to the symmetry axis [27]. The energy spacing between the band member of spin I and the bandhead is given by $\Delta E(I) = \hbar^2/2\Im\,[I(I+1) - K(K+1)]$.

The 279-keV level in ^{249}Fm decays to the ground state and to two excited states at 58 keV and 129 keV, respectively. If these states are interpreted as being the first members of the ground-state rotational band, values of $\hbar^2/2\Im = 6.6(1)$ keV and $K = 3.4(3)$ can be obtained. A ground state with $K = 7/2$ fits well with the systematics of $N = 149$ isotones (shown in Fig. 7) for which the $7/2^+[624]$ Nilsson state is or is expected to be the ground state. Furthermore, as mentioned in the Introduction, the predicted magnetic moment of such a neutron configuration [28] is the most favorable in the region for the observation of cross-over $\Delta I = 2$ transitions such as the 129-keV transition (for which the associated gyromagnetic

factor g_k is positive whereas it is negative for the other orbitals lying close to the Fermi surface). By using the theoretical total conversion coefficient for the 150-keV transition and the experimentally determined $LMN+$-conversion coefficient of the 129-keV transition, a ratio of 1.6(0.3) is obtained for the $M1/E2$ intensity ratio at the $11/2^+$ level of the ground-state band. If the theoretical conversion coefficient for the 129-keV transition is used, a ratio of 0.4(0.4) is extracted. By assuming an axial elongation of $\beta = 0.27$ for ^{249}Fm, these values correspond to the gyromagnetic factors $g_K = +0.2$ and $g_K = +0.3$, respectively. These numbers compare well with $g_k = +0.25$, which is obtained for the $7/2^+[624]$ configuration with the model of Ref. [29]. A negative gyromagnetic factor would lead to an intensity ratio greater than 6.

Since the $E1$ nature of the 279-keV transition, which decays to the $7/2^+$ ground state of ^{249}Fm, has been established, the 279-keV level must have negative parity. This negative-parity state also decays via a firmly established $E1$ transition to the second member of the ground-state rotational band with spin 9/2 and its decay to the third member of spin 11/2 is also of $E1$ nature. The 279-keV level must therefore be a $9/2^-$ state and is assigned a $9/2^-[734]$ configuration because it is the only $9/2^-$ neutron single-particle state in this region. Since the α decay of ^{253}No strongly favors this $9/2^-$ state, the ground state of ^{253}No must also have a $9/2^-[734]$ configuration. This is indeed what is predicted by most models [28–30] and follows the trend of the $N = 151$ isotones.

From systematics of the $N = 149$ isotones, one expects the presence of a low-lying $5/2^+[622]$ hole state. In ^{243}Pu, ^{245}Cm, and ^{247}Cf, this state is sizeably populated in the α decay of the respective parent nuclei (2.0%, 3.3%, and 1.8%, respectively [31]) and decays to the $7/2^+$ ground state via an $M1$ transition. Our interpretation of the available data is that the 211-keV transition corresponds to this $M1$ transition. The results obtained in this work are summarized in the decay scheme of Fig. 8.

The decay intensity out of the $5/2^+$ state represents 4.9(1.5)% of the decay intensity out of the $9/2^-$ state. To obtain estimates of the magnitude of the hindrance factors for the α decay to the $9/2^-$ and $5/2^+$ states, two approximations need to be made. First, the fraction of the intensity out of the $9/2^-$ state that comes from the feeding from the $11/2^-$ state (which should be populated in the α decay of ^{253}No but whose decay we do not observe in this experiment) is neglected. Second, roughly half the intensity out of the $5/2^+$ state is taken to come from feeding from the other members of the $5/2^+[622]$ band, as is the case in the other isotones. In these conditions, the hindrance factors are found to be 1.2(0.5) for the $9/2^-$ state and 82(25) for the $5/2^+$ state in the case of 80(20)% α branching ratio, 90% feeding of the $9/2^-$ state, and a Q value of 8.4(2) MeV. The hindrance factors for the $\Delta l = 2\hbar$ and $\Delta\pi = -1$ α decay to the $5/2^+$ state in the lighter isotones are 365 (^{243}Pu), 237 (^{245}Cm), and 207 (^{247}Cf). One would therefore expect a hindrance factor above 100 in ^{249}Fm. However, there is experimental evidence for a much more significant β-decay branch in ^{253}No [32] than the currently tabulated value, and this will have the effect of increasing the hindrance factors.

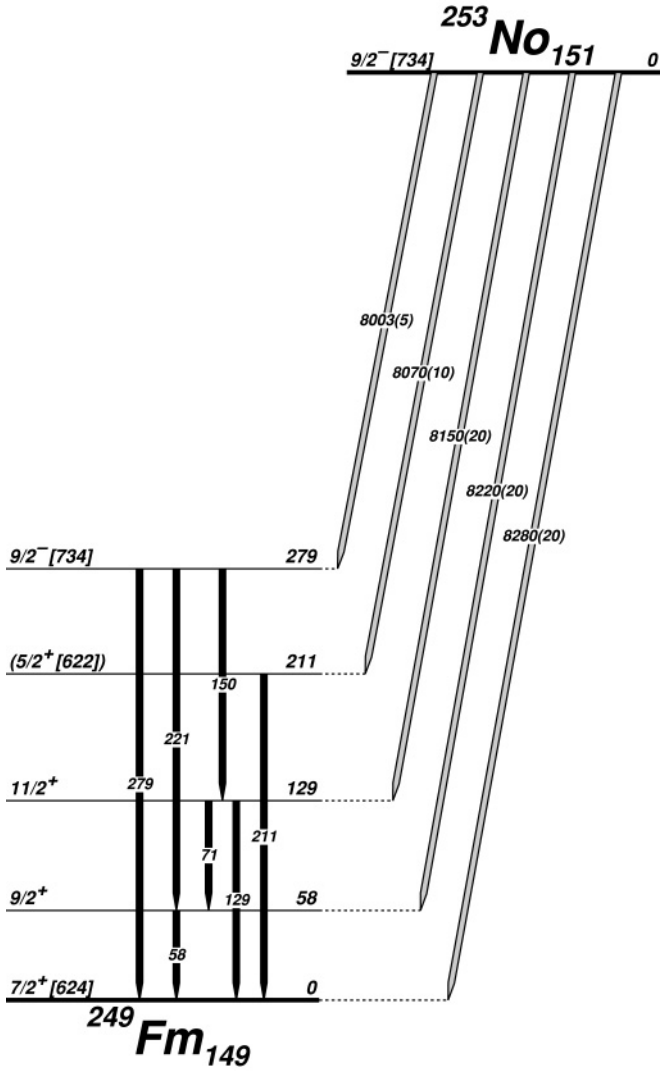

FIG. 8. Partial level scheme of ^{249}Fm sampled in the α decay of ^{253}No.

Most theoretical models predict that the first excited states in ^{249}Fm are the $9/2^-$ and $5/2^+$ states. However, the predicted ordering of these states and the excitation energy of the $5/2^+$ state do not correspond to what is found experimentally. The situation is even more flagrant in the $N = 151$ isotones ^{247}Cm and ^{249}Cf, where, even with two neutrons more, the $5/2^+$ hole excitation is still experimentally found to be the first excited state above the $9/2^-[734]$ ground state, below the $7/2^+[624]$ excited state. Some of the properties of the $5/2^+$ state, and in particular its low excitation energy, have been interpreted as a consequence of the presence of a low-lying $K = 2^-$ octupole phonon state. This state, which has been observed at a record low excitation energy of 593 keV in ^{248}Cf [33], is viewed as the superposition of two quasiparticle states, mainly the $\{7/2^+[633]\pi \otimes 3/2^-[512]\pi\}$ and $\{5/2^+[622]\nu \otimes 9/2^-[734]\nu\}$ configurations [34]. The coupling of the $K = 2^-$ phonon with the $9/2^-$ particle state gives rise to a particle-phonon $5/2^+$ state, which interacts with the $5/2^+$ hole state and pushes it down to lower excitation energies. Through this interaction, the $5/2^+$ state acquires a phonon content, which

has been inferred from the measured $B(E3)$ value to the $9/2^-$ state in ^{247}Cm [35] and measured with the (d, d') reaction in ^{249}Cf [33]. Octupole vibration-particle mixing together with Coriolis mixing may explain why the observed $E1$ branching ratios from the $9/2^-$ state to the members of the ground-state rotational band are found to strongly violate Alaga's rules [36]. Such mixing may also be responsible for an increased hindrance of the 279-keV $E1$ γ transition, which in turn leads to anomalous internal conversion.

In conclusion, excited states in ^{249}Fm have been populated and characterized by means of combined α, γ, and conversion-electron spectroscopy. The first members of the rotational band built on the $7/2^+[624]$ ground state have been observed, as well as an excited $9/2^-$ state at 279 keV and a $5/2^+$ state at 211 keV. The resulting partial level scheme is found to follow the systematics of the $N = 149$ isotones. The data suggest that the 279-keV $9/2^-[734] \rightarrow 7/2^+[624]$ transition has anomalous $E1$ K- and LMN+-conversion coefficients. This phenomenon also occurs in the lighter isotones ^{245}Cm and ^{247}Cf, which have been studied with more statistics and with better electron-energy resolution, and needs further investigation.

ACKNOWLEDGMENTS

The GABRIELA project is jointly funded by JINR (Russia) and IN2P3/CNRS (France). Work at FLNR was performed partially under the financial support of the Russian Foundation for Basic Research, Contract No. 05-02-16198 and JINR-BMBF (Germany), JINR-Polish, and JINR-Slovak Cooperation Programmes. Financial support from the Norwegian Research Council is acknowledged.

[1] R. B. Firestone, V. S. Shirley, C. M. Baglin, S. Y. F. Chu, and J. Zipkin, *Table of Isotopes*, 8th ed. (John Wiley & Sons, New York, 1996).
[2] C. E. Bemis Jr. *et al*., Chemistry division annual progress report, ORNL-4706 UC4-Chemistry (1971) 62.
[3] F. P. Hessberger *et al*., Eur. Phys. J. A **12**, 57 (2001).
[4] F. P. Hessberger *et al*., Eur. Phys. J. A **22**, 417 (2004).
[5] I. Ahmad, R. R. Chasman, and P. R. Fields Phys. Rev. C **61**, 044301 (2000).
[6] P. Reiter *et al*., Phys. Rev. Lett. **95**, 032501 (2005).
[7] I. Y. Lee, Nucl. Phys. **A520**, c641 (1990).
[8] C. N. Davies *et al*., Nucl. Instrum. Methods Phys. Res. B **70**, 358 (1992).
[9] P. Greenlees *et al*., Eur. Phys. J. A **25**, s1599 (2005); A. Chatillon *et al*., Ph.D. thesis, University of Lyon I-Claude Bernard, France (2005).
[10] P. T. Greenlees *et al*., Fusion06, AIP Conference Proceedings, Vol. 853, 416 (2006).
[11] M. Leino *et al*., Nucl. Instrum. Methods Phys. Res. B **99**, 653 (1995).
[12] R.-D. Herzberg,J. Phys. G **30**, R123 (2004).
[13] M. Asai *et al*., Phys. Rev. Lett. **95**, 102502 (2005).
[14] O. N. Malyshev *et al*., Nucl. Instrum. Methods Phys. Res. A **440**, 86 (2000).
[15] O. N. Malyshev *et al*., Nucl. Instrum. Methods Phys. Res. A **516**, 529 (2004).
[16] K. Hauschild *et al*., Nucl. Instrum. Methods Phys. Res. A **560**, 388 (2006).
[17] I. Rezanka *et al*., Phys. Rev. C **10**, 766 (1974).
[18] S. Agostinelli *et al*., Nucl. Instrum. Methods Phys. Res. A **506**, 250 (2003).
[19] M. O. Krause, J. Phys. Chem. Ref. Data **8**, 307 (1979).
[20] S. I. Salem, S. L. Panossian, and R. A. Krause, At. Data Nucl. Data Tables **14**, 91 (1974).
[21] R. S. Hager and E. C. Seltzer, Nucl. Data A **4**, 1 (1968).
[22] O. Dragoun, H. C. Pauli, and F. Schmutzler, Nucl. Data A **6**, 235 (1969).
[23] I. M. Band, B. Trzhaskovskaya, C. W. Nestor, P. O. Tikkanen, and S. Raman At. Data Nucl. Data Tables **81**, 1 (2002).
[24] R. R. Chasman, I. Ahmad, A. M. Friedman, and J. R. Erskine, Rev. Mod. Phys. **49**, 833 (1977).
[25] S. G. Nilsson and J. Rasmussen, Nucl. Phys. **5**, 617 (1958).
[26] E. L. Church and J. Weneser, Annu. Rev. Nucl. Sci. **10**, 193 (1960).
[27] A. Bohr and B. R. Mottelson, *Nuclear Structure*, Vol. 2 (W. A. Benjamin Inc., New York, 1969).
[28] M. Bender *et al*., Nucl. Phys. **A723**, 354 (2003).
[29] S. Cwiok, S. Hofmann, and W. Nazarewicz, Nucl. Phys. **A573**, 333 (1994).
[30] A. Parkhomenko and A. Sobiczewski, Acta Phys. Pol. **B36**, 3115 (2005).
[31] A. Rytz At. Data Nucl. Data Tables **47**, 205 (1991).
[32] P. T. Greenlees, communication at the Midwinter Exotag Workshop on tagging methods and experiments, January 2005 http://www.phys.jyu.fi/research/gamma/exotag/greenlees.pdf.
[33] S. W. Yates, R. R. Chasman, A. M. Friedman, I. Ahmad, K. Katori, Phys. Rev. C **12**, 442 (1975).
[34] V. G. Soloviev and T. Siklos, Nucl. Phys. **59**, 145 (1964).
[35] I. Ahmad *et al*., Phys. Rev. C **68**, 044306 (2003).
[36] G. Alaga, K. Adler, A. Bohr, and B. R. Mottelson, K. Dan. Vidensk. Selsk. Mat.-Fys. Medd. **29**, (9) (1955).